Nitrate-dominated PM$_{2.5}$ and elevation of particle pH observed in urban Beijing during the winter of 2017

Yuning Xie [1], Gehui Wang [1,2] *, Xinpei Wang [1], Jianmin Chen[2,3], Yubao Chen [1], Guiqian Tang [4], Lili Wang [4], Shuangshuang Ge [1], Guoyan Xue [1], Yuesi Wang[4], Jian Gao[5]

[1]Key Laboratory of Geographic Information Science of the Ministry of Education, School of Geographic Sciences, East China Normal University, Shanghai 200241, China

[2]Institute of Eco-Chongming, 3663 N. Zhongshan Rd., Shanghai 200062, China

[3]Department of Environmental Science and Technology, Fudan University, Shanghai, China

[4]State Key Laboratory of Atmospheric Boundary Layer Physics and Atmospheric Chemistry, Institute of Atmospheric Physics, Chinese Academy of Sciences, Beijing 100080, China

[5]Chinese Research Academy of Environmental Sciences, Beijing 100000, China;

Correspondence to: Prof. Gehui Wang (ghwang@geo.ecnu.edu.cn)

Abstract: Chinese government has exerted strict emission controls to mitigate air pollution since 2013, which resulted in significant decreases in the concentrations of air pollutants such as SO$_2$, NOx and PM$_{2.5}$. To investigate the impact of such changes on the chemistry of atmospheric aerosols in China, we conducted a comprehensive characterization on PM$_{2.5}$ in Beijing during the winter of 2017. Strict pollution control actions also reduced the average PM$_{2.5}$ concentration to a low level of 39.7 μg m^{-3} in urban Beijing during the winter of 2017. Compared with the historical record (2014–2017), SO$_2$ decreased to a low level of 3.2 ppbv in the winter of 2017 but NO$_2$ level was still high (21.4 ppbv in the winter of 2017). Accordingly, contribution of nitrate (23.0 μg m^{-3}) to PM$_{2.5}$ far

exceeded over sulfate (13.1 μg m^{-3}) during the pollution episodes, resulting in a significant increase of nitrate to sulfate molar ratio. The thermodynamic model (ISORROPIA-II) calculation results showed that during the PM$_{2.5}$ pollution episodes particle pH increased from 4.4 (moderate acidic) to 5.4 (more neutralized) when the molar ratio of nitrate to sulfate increased from 1 to 5, indicating that aerosols were more neutralized as the nitrate content elevated. Based on the results of sensitivity tests, the future prediction for the particle acidity change was discussed. We found that nitrate-rich particles in Beijing at low and moderate humid conditions (RH: 20%–50%) can absorb twice amount of water than sulfate-rich particles, and the nitrate and ammonia with higher levels have synergetic effects, rapidly elevating particle pH to merely neutral (above 5.6). As moderate haze events might occur more frequently under the abundant ammonia and nitrate-dominated PM$_{2.5}$ conditions, the major chemical processes during haze events and the control target should be re-evaluated to obtain the most effective control strategy.

1 Introduction

Severe haze pollution has been causing serious environmental problems and harming public health in China over the past decades (He et al. 2001; Wang et al. 2016; Zhang et al. 2015b). Therefore, strong actions have been taken to improve the worsening atmospheric environment, including cutting down the pollutant emissions with forced installation of catalytic converter on vehicles, building clean-coal power generation system, prohibiting open burning of crop residue during the harvest seasons, etc. (Chen et al. 2017; Zhang et al. 2012; Liu et al. 2016). As a result, the PM$_{2.5}$ pollution is relieved to meet the goals in Air Pollution Prevention and Control Action Plain (issued by the State Council of China, http://www.gov.cn/zwgk/2013-09/12/content_2486773.htm, in Chinese). Among all the regions of interests, Beijing has achieved great success in PM$_{2.5}$ reduction (the annual average PM$_{2.5}$ concentration of 2017 was 58 μg m^{-3}). Yet, PM$_{2.5}$ concentration in Beijing is still higher than that in most developed countries.

There are many factors contributing to the PM$_{2.5}$ pollution in China (Guo et al. 2014; Ding et al. 2013). The PM$_{2.5}$ pollution across the country is featured by significantly high secondary formation of inorganic components

(Huang et al. 2014a). Sulfate, nitrate and ammonium (SNA) comprised over 30% of the $PM_{2.5}$ mass, and SNA's

45   fraction continues to increase during the pollution evolution (Cao et al. 2012). While models could well predict the airborne particle pollution in the U.S. or Europe, it is challenging to simulate the real atmospheric pollution in China (Wang et al. 2014; Ervens et al. 2003). Previous modeling works showed that the simulated $PM_{2.5}$ concentrations were underestimated within the current scheme, which is related to the important role of heterogeneous reactions in the SNA formation processes (Huang et al. 2014b; Herrmann et al. 2005). It was reported that the classical formation

50   mechanism of sulfate in the atmosphere was through oxidation by H_2O_2, but recent studies in China pointed out that non-classical H_2O_2 formation pathways, which are mentioned in text books, cannot be ignored. In Beijing, severe haze events occur with abundant nitrogen species (NO_x, NH_3, etc.), high relative humidity (RH) and less active photochemistry (Wang et al. 2016; Cheng et al. 2016). Field observations, chamber experiments, source apportionments and numerical simulation works all suggest that the joint effect of NO_2, SO_2, and NH_3 is important

55   for the sulfate formation processes in haze events (Cheng et al. 2016; Wang et al. 2016; Wang et al., 2018; He et al. 2018, Xue et al., 2019). Aqueous oxidation of SO_2 by NO_2 could be a major process of sulfate formation in Beijing during winter, as well as the catalyzed oxidation by transition metal ions (TMI) (Wang et al. 2016; Cheng et al. 2016). Besides, although the photochemistry is less active during haze periods in winter, the extra OH radical provided by HONO might enhance the atmospheric oxidation capacity and lead to a rapid formation of SNA (Tan et

60   al. 2018, Ge et al. 2019). Since these reactions are all sensitive to particle acidity, adequate quantification of airborne particles' acidity is essential for elucidating the specific contribution.

Particle acidity has been widely studied due to its important role in the haze formation, and has been widely implemented in major models (Yu et al. 2005; Robert et al. 2016). Since the practical method of directly measuring the particle acidity in real atmosphere is not available (Wei et al. 2018; Freedman et al. 2019), thermodynamic

65   models, which can calculate the particle pH, have been mostly used in quantifying the particle acidity. Most models (ISORROPIA II, E-AIM-IV, AIOMFAC, etc.) can predict H^+, aerosol liquid water content (ALWC) and the partitioning of volatile/semi volatile components, such as ammonia (Fountoukis and Nenes 2007; Clegg et al. 2008).

These models' abilities to describe physiochemical properties of airborne particles have been validated in various studies (Weber et al. 2016; Guo et al. 2016; Shi et al. 2017; Tao and Murphy 2019; Murphy et al. 2017). However,

70 several publications using the same method gave different particle pH values in Beijing, and contradictory conclusions were drawn on the importance of the sulfate formation by NO_2 oxidation. Cheng et al. (2016) conducted some modeling work and suggested that the $PM_{2.5}$ pH in Beijing ranges between 5.4 and 6.2, which is favorable for the aqueous NO_2 oxidation. The NO_2 oxidation's major contribution and the importance of high ALWC and sufficient ammonia are supported not only by modeling works, but also by field observation and chamber study

75 (Wang et al. 2016; Chen et al. 2019). On the contrary, Liu et al. (2017) simulated the particle pH during the winter of 2015 and 2016 with the same method, and claimed that pH of the Beijing haze particles was lower (3.0–4.9, average 4.2) and unfavorable for the NO_2 oxidation mechanism. Based on the ISORROPIA-II model results , which assumed Chinese haze particles as a homogeneous inorganic mixture, Guo et al. (2017) further concluded that high ammonia cannot raise the particle pH enough for the aqueous oxidation of SO_2 by NO_2. Recently Song et al. (2018)

80 reported that the thermodynamic model (ISORROPIA-II) has coding errors, which can lead to the predicted pH values negative or above 7. Furthermore, with lab studies and field observations, Wang et al. (2018) raised the concern that whether it is appropriate to elucidate sulfate production for the Beijing haze by using particle pH predicted only based on the inorganic compositions. In fact, since the real atmosphere is affected by uncountable factors, it is common that particle pH has variation when simulated with the ambient data. Although the pH

85 predicted by the thermodynamic models are of uncertainty, it is widely believed that haze particles in China are moderate acidic and are more neutralized than those in the US., given that the gaseous ammonia is still at a high level relative to particulate ammonium(Song et al. 2018).

Air pollution control in China has entered the second phase—further mitigation of the moderate haze pollution, which is characterized by high levels of nitrate and ammonium and low level of sulfate (Liu et al. 2019; de Foy et al.

90 2016) due to the efficient SO_2 emission control. Such a change in chemical compositions could significantly alter physicochemical properties of the atmospheric aerosols in China. This paper aims to investigate the variation of the

particle acidity of $PM_{2.5}$ when the sulfur emission was well controlled in Beijing. First, the compositions of air pollutants, including inorganic components of $PM_{2.5}$ during the winter of 2017 and 2018, were analyzed and compared with previous studies; then, based on observations, the response of particle acidity to the elevation of

95   nitrate was studied by using the ISORROPIA II thermodynamic model; and finally, the possible changes in the future are discussed based on the sensitivity tests.

2 Sampling site and instrumentation

The observation was conducted at an urban site—the State Key Laboratory of Atmospheric Boundary Layer Physics and Atmospheric Chemistry, Institute of Atmospheric Physics (IAP), Chinese Academy of Sciences

100   (39°58′28″N, 116°22′16″E) in Beijing. All the instruments were on the roof of a two-story building. The local emissions are mainly from the vehicles, and the industrial emission is greatly reduced since the major factory/power plants are moved out of Beijing or phased out due to the emission control policy. Overall, this site represents the typical atmospheric environment of urban Beijing, from which the data obtained can be compared with those from previous studies in the city (Ji et al. 2018).

105   A continuous online measurement of atmospheric components was conducted with a time resolution of 1 hour. Two $TEOM^{TM}$ continuous ambient PM monitors using $PM_{2.5}$ or PM_{10} cyclone inlet (Metone) were applied to obtain $PM_{2.5}$ and PM_{10} mass concentrations. For trace gases (O_3, NO_2 and SO_2), a series of gas monitors were used for the hourly measurement (Model 49i, 42i and 43i, respectively). Meteorology data, including ambient temperature, RH, wind speed, wind direction and total solar radiation, were measured with an automatic weather station (MILOS 520,

110   VAISALA Inc., Finland) located in the middle of the observation site yard. Visibility data of Beijing were downloaded from the website of https://gis.ncdc.noaa.gov/maps/ncei/cdo/hourly. Apart from these online monitors, a high-volume sampler (TISCH ENVIRONMENTAL) with a $PM_{2.5}$ inlet was used to collect $PM_{2.5}$ samples on a day/night basis (daytime of 8:00–17:50 and nighttime of 18:00–7:50).

The inorganic water-soluble components of $PM_{2.5}$ (SO_4^{2-}, NO_3^-, Cl^-, NH_4^+, Na^+, Ca^{2+}, Mg^{2+} and K^+) and

ammonia gas were measured with an online-IC system: IGAC (In-situ Gases and Aerosol Composition monitor, Fortelice International Co., Ltd.). IGAC comprises of 2 parts: sampling unit and analyzer unit (Young et al. 2016). A vertical wet annular denuder (WAD) is used to collect the gas-phase species prior to a scrub and impactor aerosol collector (SIC), while the latter part can efficiently collect particles into liquid samples. During the campaign, 1mM H_2O_2 solution is used as the absorption liquid for the air samples. Under most atmospheric conditions, the absorption liquid can well absorb the target atmospheric components (e.g. SO_2). An ICS-5000$^+$ ion chromatograph is used as the analyzer unit in this study. For anions, an AS18 column (2 mm $\times$ 250 mm, Dionex™ IonPac™) is used while a CS-16 column (4 mm $\times$ 250 mm, Dionex™ IonPac™) is chosen to analyze major cations, both running with recommended eluent (solution of KOH for anion/methane sulfonic acid for cation). The performance of the system has been tested and improved over recent years, and studies of $PM_{2.5}$ water-soluble ion observations have been conducted by using it (Young et al. 2016; Song et al. 2018; Liu et al. 2017). A better sensitivity due to the advanced suppression technology of the system greatly enhances its ability to measure trace ions, such as sodium and magnesium, which is important in studies of particle ion balance. For details of the comparison between IGAC and filter sampling results, please refer to supplementary materials (Fig. S1).

3. Results

3.1 Major pollutants' levels

We firstly present the overall time series and statistics of major pollutants and meteorological parameters from Dec. 15th, 2017 to Feb. 25th, 2018. As shown in Fig.1, during the observation campaign, Beijing was relatively cold and dry. Due to the frequent cold-air outbreaks, the average air temperature was around 0℃, with a minimum of −10℃, and the RH was low on average (20%–30%) with a maximum of 80%. The average total solar radiation was 254.3 w m^{-2}, which is typical in Beijing during winter. The wind usually blew from the north with an average speed of 1.9 m s^{-1}, but the strong wind (over 5 m s^{-1}) frequently occurred on the clean days. Benefiting from the weather condition, the atmospheric pollution in Beijing was much weaker than that in the winter of 2013. Overall, the

improvement of the atmospheric environment was visible: the average visibility was around 15 km during the campaign and about 7.5 km during the pollution periods.

140   With strict control actions, there were less $PM_{2.5}$ pollution episodes and its concentration kept at a low level during most of the time in the winter of 2017. The average concentrations of $PM_{2.5}$ and PM_{10} were 39.7 µg m^{-3} and 68.5 µg m^{-3}, respectively. According to the $PM_{2.5}$ concentration, three conditions of the atmospheric environment were classified in this study : clean (the $PM_{2.5}$ was below 35 µg m^{-3}), transition (the $PM_{2.5}$ was between about 35 µg m^{-3} and 75 µg m^{-3}) and pollution (the $PM_{2.5}$ was above 75 µg m^{-3}). In the clean, transition and pollution periods, the

145   average $PM_{2.5}$ concentrations were 13.0±7.8 µg m^{-3}, 52.0±11.4 µg m^{-3} and 128.0±46.5 µg m^{-3} , respectively (as showed in Table 1), indicating that there was still $PM_{2.5}$ pollution during the winter, with a maximum hourly $PM_{2.5}$ concentration of 298 µg m^{-3}. The average ozone concentration was 18.5±12.8 ppbv, and the value decreased as $PM_{2.5}$ concentrations increased. The average SO_2 concentration (3.2±3.1 ppbv) was almost 10 times lower than that of NO_2 (21.4±14.8 ppbv). The significant gap between SO_2 and NO_2 concentrations can be attributed to the sulfur

150   emission control over recent years and the fast increase of gasoline vehicles in Beijing (Cheng et al. 2018; Wang et al. 2018b). Both gaseous pollutants showed an increasing trend as the $PM_{2.5}$ concentration increased during the haze episodes, but the increase of NO_2 was much more significant.

NO_2 and SO_2 are the most important precursor gases for major secondary inorganic nitrate and sulfate in $PM_{2.5}$. Due to the emission control, the sulfur emission decreased significantly, resulting in lower ambient SO_2

155   concentration. To better describe it, changes of these two precursor gases during winter are investigated by examining the data from 2014 to 2016 in Beijing. Average values and the standard deviation are plotted in Fig. 2. SO_2 showed a significant decreasing trend in all the three periods. In 2014, SO_2 in the three periods were 3.9, 10.0 and 16.9 ppbv, respectively. The SO_2 concentration difference in different conditions was narrowing. Until 2017, the difference of SO_2 concentrations between any two of three conditions had been all within 10 ppbv. Meanwhile, NO_2

160   concentrations kept increasing after 2015 in clean and transition conditions, but the NO_2 concentration   during the pollution periods of 2017 was surprisingly lower than that in 2014. Although the dilution condition was much better

than before, more quick and strong actions were taken to prevent the $PM_{2.5}$ pollution in 2017, such as construction prohibition, private vehicle restriction and vast shutting down of factories in neighboring regions (Cheng et al. 2018). The significant drop of NO_2 proves the effectiveness of pollution control in 2017.

165 **3.2 $PM_{2.5}$ chemical compositions**

According to several previous reports, the chemical compositions of $PM_{2.5}$ during the winter of 2017 in Beijing changed significantly (Shao et al. 2018; Elser et al. 2016; Ge et al. 2017; Huang et al. 2017; Wang et al. 2017). The major inorganic ions of $PM_{2.5}$ in Beijing during the winter of 2017 included ammonium (3.3 ± 4.4 μg m^{-3}), nitrate (7.1 ± 9.6 μg m^{-3}), sulfate (4.5 ± 5.9 μg m^{-3}) and chloride (2.4 ± 2.3 μg m^{-3}).   Concentrations of the major components

170 increased as the $PM_{2.5}$ concentration increased, but changes in the crustal ion (Na^+, Mg^{2+} and Ca^{2+}) concentrations were less significant among the clean, transition and pollution periods. K^+ increased during the $PM_{2.5}$ pollution episodes (average concentration: 2.3 ± 5.1 μg m^{-3}), indicating the possible contribution of biomass burning sources or fireworks during Chinese New Year. Cl^- in $PM_{2.5}$ has been used as a tracer for biomass burning and the coal consumption. The concentration of Cl^- in $PM_{2.5}$ chloride increased significantly as $PM_{2.5}$ increased, but the

175 imbalance of chloride molar concentration to potassium suggests that biomass burning might not be the major source of $PM_{2.5}$ chloride other than the coal consumption during the $PM_{2.5}$ pollution episodes in Beijing.

SNA greatly increased the $PM_{2.5}$ pollution. Unlike the findings from some previous studies (Wang et al. 2016; Huang et al. 2014a; Ji et al. 2014), nitrate dominated the water-soluble ions (WSIs) in the winter of 2017. During pollution episodes, concentration of nitrate and sulfate were respectively 23.0 ± 10.7 μg m^{-3} and 13.1 ± 8.4 μg m^{-3},

180 with an average molar ratio of nitrate to sulfate (Ratio $_{N-to-S}$) around 3.3 ± 1.4. Fig.3 shows the correlation of nitrate and sulfate with the total water-soluble ions. Sulfate presented a lower fraction when total WSIs was below 65 μg m^{-3}, but the fraction increases as WSIs exceeds 65 μg m^{-3}, showing an enhanced formation of sulfate during heavy pollution episodes. Interestingly, the ratio of nitrate to WSIs remained the same throughout the campaign. As the concentrations of other components also increased, this phenomenon indicated that the nitrate formation was

185 enhanced in hazy days. Besides, the concentrations of ammonium and ammonia both increased significantly (from

0.9 μg m^{-3} to 10.4 μg m^{-3}) from the clean to the pollution condition.

3.3 Comparison of major inorganic compositions during the early 21st century in Beijing

To illustrate the changes in chemical compositions of PM$_{2.5}$ at the China's economy booming stage

(1999–2017), nitrate, sulfate and ammonium are chosen for the comparison with previously reported data during

190 winter in Beijing (Fig. 4). Only winter-averaged observation data or representative pollution records are selected to

show the significant change of SIA compositions. On average, although the concentration might be varied due to

different emissions and weather conditions over the years, SIA concentration in the winter of 2017 was the lowest

compared with the years before. Sulfate concentration varied from 4.5 μg m^{-3} to 25.4 μg m^{-3} and contributed the

most PM$_{2.5}$ masses among SIA species during the pollution episodes before 2015. The emission control of SO$_2$

195 started in 2006 to prevent adverse atmospheric environment events such as acid rain and high particulate matter

loading (Wang et al. 2013; Wang et al. 2018b). As a result, the sulfate concentration in winter decreased gradually

(see results of 1999, 2011, 2015-a and 2017), the average concentration in recent years has been much lower than

that in the early 2000s (detailed literature comparison can be found in Lang et al. (2017)). However, it was widely

reported that sulfate still contributed the most to the PM$_{2.5}$ mass concentration during the severe haze periods, such

200 as the winter of 2013 (Huang et al. 2014a; Guo et al. 2014; Ji et al. 2014). The heterogeneous formation might be

responsible for the enhanced conversion ratio from SO$_2$ to particulate sulfate, including the NO$_2$-promoted aqueous

reaction and transition-metal-catalyzed oxidations (Huang et al. 2014b; Xie et al. 2015). On the other hand, the NO$_x$

emission in North China significantly increased as the power consumption and transportation kept increasing.

Therefore, nitrate in PM$_{2.5}$ had been increasing since 2011. The average concentration of nitrate rose from 7.1 μg m^{-3}

205 to 29.1 μg m^{-3}. By 2015, the nitrate concentration had exceeded the sulfate concentration, and the two equally

contributed to PM mass in winter pollution episodes. Although the nitrate concentration during pollution periods

decreased in 2017 (23.0 μg m^{-3}), the decrease was not significant and the concentration was still comparable to

previous studies. The winter-averaged ammonium concentration reached the maximum (~20 µg m^{-3}) in 2015, but decreased afterwards. The decreasing trend of ammonium, which is the major neutralizer in the atmosphere of

210   Beijing, well represented the efficient pollution control of SNA compositions during the winter of 2017. In a word, as the dominant composition, high nitrate fraction has become one of the major features of PM$_{2.5}$ in Beijing during winter.

The ratio between major SIA components can better represent the composition change discussed above. As shown in Fig.5, the nitrate to sulfate ratio (Ratio$_{N-to-S}$) has been increasing significantly from below 1.0 to 2.7 (1999

215   vs. 2017). Ratio$_{N-to-S}$ was around 1 before 2013 but then steadily increased after 2013, same as previous publications (Shao et al. 2018; Lang et al. 2017). Interestingly, Ratio$_{N-to-S}$ during pollution episodes was lower than the winter average in 2015, but Ratio$_{N-to-S}$ during pollution episodes greatly exceeded the average in 2017, showing the dominance of nitrate in the present PM$_{2.5}$ pollution. The rapid increase of Ratio$_{N-to-S}$ not only resulted from the sulfur emission control, but also from more nitrate partitioning to the particle phase. Abundant ammonia in the Beijing

220   atmosphere can enhance the partitioning of nitric acid gas by forming ammonium nitrate. To identify whether the ammonia is sufficient, the ammonium to sulfate ratio (Ratio$_{A-to-S}$) is calculated with the published data as well. It is reported that North China Plain experienced ammonia insufficiency during summer (Ratio$_{A-to-S:}$ less than 1.5), limiting the formation and partitioning of nitrate into the particle phase (Pathak et al,. 2004; Pathak et al. 2009; Pathak et al. 2011). However, Ratio$_{A-to-S}$ in Beijing during winter was always above 1.5. The lowest value appeared

225   in 1999 (averaged Ratio$_{A-to-S}$: 1.7), then the ratio increased rapidly (above 3) after 2011 (red bars in Fig.5). In recent years, the Ratio$_{A-to-S}$ has reached around 4. This value is typically observed in the eastern America during winter, though the absolute concentration is much higher in Beijing (Shah et al. 2018). To sum up, the effective sulfur emission control and ammonia-rich atmosphere provide the favorable environment for nitrate formation, and eventually change PM$_{2.5}$ in Beijing from sulfate-dominated to nitrate-dominated type.

 3.4 Aerosol pH's response to the elevation of nitrate fraction in PM$_{2.5}$

The shift from sulfate-dominated to nitrate-dominated PM$_{2.5}$ further influences the secondary chemical processes via changing physiochemical properties of aerosols, e.g. hygroscopicity and particle acidity. In a thorough study in the U.S, despite the well control of NO$_x$ emission, the nitrate fraction in PM$_{2.5}$ didn't show a corresponding decreasing trend. It was caused by the elevated partitioning of nitric acid to the particle phase in the eastern America (Shah et al. 2018). Researchers implied that higher nitrate partition fraction is resulted from the increasing particle pH, while some studies showed that the particle pH was decreasing as particulate sulfate decreases in the U.S (Weber et al. 2016). Since the chemical composition of PM$_{2.5}$ changed significantly, it is necessary to study the relevant response of particle acidity based on high-resolution observation datasets.

In this study, the bulk particle pH is calculated with the thermodynamic model ISORROPIA II in forward mode with the assumption of aerosol in metastable state. The simulation is limited to the data with the corresponding RH between 20%–90%, same as that in previous studies (Liu et al. 2017; Cheng et al. 2016). The analysis is further limited to data with sufficient ALWC (above 5 μg m^{-3}) to avoid unrealistic pH values caused by false predictions of ALWC. To study the effect of the nitrate fraction's elevation on particle acidity, the Ratio$_{N-to-S}$ is compared to the bulk particle pH (Fig. 6). As the nitrate fraction increases, the particle pH increases. When the ratio is between 0–2, predicted pH values are rather scattered (2.1~6.2) with a median value of 4.4. As the ratio increases, pH values become less scattered and the median value increases as well. When the ratio is around 4–6, the predicted pH values range from 4.9 to 5.6 with a median value of 5.4, which is comparable with previous reported values in PM$_{2.5}$ pollutions (Cheng et al. 2016; Wang et al. 2016; Xie et al. 2015). There are several factors causing the chemistry nature of the pH increasing with higher Ratio$_{N-to-S}$, including neutralization by ammonia, higher pH of ammonium nitrate in comparison with ammonium sulfate, and increased ALWC leading to dilution of predicted H$^+$ (Hodas et al. 2014; Xue et al. 2014; Wang et al. 2018c). To confirm that the pH elevation is not caused by crustal ions, the simulation using data without crustal ions (input is set to 0) was conducted. It is shown that the exclusion of crustal ions in the simulation can cause an overall lower pH, but the pH elevation with Ratio$_{N-to-S}$ is still observed

(detailed analysis can be found in the supplementary materials, Figs. S2 and S3).

255   In this study, fewer predicted H^+ ions in aerosol liquid water were found to be the major cause of the higher pH with high nitrate fraction. The correlation between H^+ and major anions (HSO_4^-, SO_4^{2-}, NO_3^-, Cl^-) is shown in Fig.7 to identify the acidity contribution of each anion. Sulfate and bisulfate have long been recognized as major acidic components of atmospheric particles. Their concentrations have significant impact on the particle acidity (Weber et al. 2016; Liu et al. 2017). Therefore, the H^+ ion concentration was found to strongly correlate with sulfate as well as

260 bisulfate (Figs. 7a and 7b). The outlier data points can be attributed to the fireworks events during the Chinese New Year (extreme data on Chinese New Year's Eve are excluded). The average molar ratio of bisulfate to sulfate is 1.08 $\times$ 10^{-6}, indicating that most of the sulfate is balanced by ammonium, same as the results reported by previous studies (Song et al. 2018). The excess ammonium is then balanced by nitrate and chloride. The correlation between H^+ and nitrate ion is much different as ALWC varies (Fig. 7c). Under the high-ALWC condition, the H^+ increases

265 with the nitrate concentration, which can be explained by the simultaneously increasing sulfate fraction during several pollution episodes. Under the drier condition (ALWC < 10μg m^{-3}), as NO_3^- increases, H^+ decreases, which implies that the weaker aerosol acidity favors nitric acid partitioning to the particle phase. Since HCl is more volatile than nitric acid gas, its occurrence in the particle phase is more sensitive to the particle acidity (Fig. 7d). Therefore, the negative correlation with H^+ is much obvious when it comes to chloride, free of ALWC amount.

270   The low level of H^+, especially its negative correlation with $Ratio_{N-to-S}$ should be attributed to the neutralization by ammonia via gas-particle partitioning. Under most conditions, the excess of ammonia is an implicit prerequisite for SIA formation in Beijing, and higher NH_3 concentration could increase the predicted particle pH (Guo et al. 2017; Weber et al. 2016). As an auxiliary evidence, ammonia partition fraction (F_{NH4}, calculated with observation data) exhibits a positive trend as $Ratio_{N-to-S}$ increases (Fig. 8), while ammonia concentration remains less varied in the

275 same case (Fig.S4). The positive trend is divided into two parts: a more acidic (pH below 4.5) branch with $Ratio_{N-to-S}$ of 1–3 and F_{NH4} of 0.1–0.6 and the other less acidic (pH above 5.5) branch with $Ratio_{N-to-S}$ of 1–7 and F_{NH4} of 0.1–0.4. The overall higher F_{NH4} in the lower pH branch is reasonable since it is more favorable for ammonia

partitioning to the particle phase when airborne particles exhibit higher acidity. Moreover, sulfate can accommodate twice amount of ammonia than nitrate and thus increase F_{NH4}. Yet, the highest value of F_{NH4} were observed with more nitrate (Ratio $_{N-to-S}$ ~2.5) and a slightly higher pH. By contrast, even though the high particle pH (5~6) can prevent ammonia from partitioning to the particle phase (Guo et al. 2017), the elevation of F_{NH4} with increasing Ratio $_{N-to-S}$ (1–4) is still observed with pH ranging 5 to 6 despite there were some outliers with lower F_{NH4} which is not caused by higher NH_3 concentration. Nitrate formation is observed to be enhanced in North China, either by heterogeneous formation (e.g. N_2O_5 hydrolysis) or with sufficient ambient NH_3 (Wang et al. 2013). The positive trend of F_{NH4} with Ratio$_{N-to-S}$ clearly shows that nitrate formation and partitioning have significant contribution to NH_3 partitioning process, and will lead to an enhanced neutralization with the help of more ammonia partitioning into the particle phase. Combining these analyses, we conclude that fine particles enriched in nitrate in Beijing during winter will lead to lower particle acidity.

4. Discussion: possible impacts of increasing fraction of nitrate in PM$_{2.5}$

So far, the effect of emission control on SNA compositions in Beijing's PM$_{2.5}$ pollution and the response of particle pH have been illustrated, but it is important to make predictions with the current knowledge for future better control strategy. In this section, sensitivity tests regarding to hygroscopicity and particle-acidity change are conducted to help understand the possible changes of these properties in the future. ALWC is directly engaged in the calculation of particle pH and limited by several major parameters (RH, hydrophilic composition concentration, temperature, etc.). During the campaign, the ALWC predicted by ISORROPIA II varied between 0.8 and 154.2 μg m^{-3} with an average value of 6.4 μg m^{-3}. As previously mentioned, the average value of Ratio$_{N-to-S}$ is around 2 during the haze events in the winter of 2017 in Beijing. The average ALWC in the haze events increased to 24.4 μg m^{-3} accordingly. It has been reported that nitrate salts have greater contribution to ALWC due to its lower deliquescence RH, and the elevated ALWC might has strong impact on water-soluble gas partitioning such as glyoxal, leading to an enhanced SOA production (Hodas et al. 2014; Xue et al. 2014). As a matter of fact, the increase of hygroscopicity

related to nitrate-rich fine particles has been observed in Beijing (Wang et al. 2018c). However, it is difficult to conclude that lower pH in nitrate-rich particles is caused by the dilution of H^+ with higher ALWC with current data, since the higher nitrate fraction is usually observed with the moderate RH in pollution episodes in the winter of 2017.

The possible enhancement of hygroscopicity in nitrate-rich $PM_{2.5}$ was investigated. Most single salts can only be deliquesced over a certain RH, thus the ALWC only exists when a certain RH is exceeded (Wexler and Seinfeld 1991; Mauer and Taylor 2010). In real atmosphere, aerosols are usually a mixture of salts and organics, which might be easier to deliquesce. In addition, the deliquescence of NH_4NO_3 is unique, and it becomes more complicated in the system of $NH_4NO_3/(NH_4)_2SO_4$. The NH_4NO_3 system would absorb water vapor even at an extreme low RH (down to 10%) (Willeke et al. 1980; ten Brink and Veefkind 1995). The system comprised of $NH_4NO_3/(NH_4)_2SO_4$ has a higher deliquesce point when the sulfate content is higher ($Ratio_{N-to-S}<1$), but absorbs water even at low RH (~20%) when nitrate is dominant ($Ratio_{N-to-S} > 2$) in $PM_{2.5}$ inorganic ions (Wexler and Seinfeld 1991; Ge et al. 1996, 1998). Inspired by these facts, we conducted a sensitivity test of ALWC to RH by using the observation dataset to study the effect of nitrate fraction elevation on ALWC changes (the RH value ranging from 20% to 90%, with 10% as interval). Concentrations of pollutants in the clean periods are relatively low and the data of the clean periods might be more influenced by the observation artifacts. Thus, only the data obtained in the transition and pollution conditions were analyzed here. The ALWC changes are defined as Eq (1).

$$Fraction_{change} = ALWC_{(RH+10\%)}/ALWC_{RH} \tag{1}$$

Then, we choose the data with $Ratio_{N-to-S}$ above 3 and $Ratio_{N-to-S}$ below 1. These values were both mentioned in previous lab studies (Ge et al. 1998) and are also typical values of nitrate-rich or sulfate-rich conditions in field observations. As shown in Fig. 9, $PM_{2.5}$ with higher $Ratio_{N-to-S}$ adsorbs more water than lower nitrate fraction as the RH increases, which is more significant under lower RH (<50%) conditions compared with that uner higher RH (50%–70%) conditions. As the RH is usually lower (30%–50) at the beginning stage of $PM_{2.5}$ pollution development in Beijing, such a significant increase in hygroscopicity of nitrate-rich particles can greatly promote the haze

formation under relatively dry conditions by enhancing the gas-to-particle partitioning of water-soluble compounds

325   and the aqueous-phase formation of secondary aerosols, e.g. ammonia partitioning and nitrate formation through

partitioning or hydrolysis of N_2O_5 (Badger et al. 2006; Bertram and Thornton 2009; Sun et al. 2018; Hodas et al.

2014; Shi et al. 2019).

The response of particle pH to ammonia and sulfate changes has been indicated in previous studies (Weber et al.

2016; Guo et al. 2017; Murphy et al. 2017). Here we further analyze the particle pH under the elevated nitrate

330   concentration with the increasing ammonia in the atmosphere, which is expected to be the case for most Chinese

cities in the coming years. Two kinds of pH sensitivity tests are conducted: one with fixed nitrate but varying sulfate

and ammonia and the other with fixed sulfate input but varying nitrate and ammonia (Fig. 10). In the test, crustal

ions were all set as 0, while fixed chloride, sulfate and nitrate concentrations were set as the average data in pollution

(see Table 2). Compared with previous studies (Guo et al. 2017; Song et al. 2018), the RH was set as 58% and the

335   temperature was set as 273.15K. Despite system errors due to the instability of the model at the extreme high-anion

and low-NH_x condition (Song et al. 2018), the pH shows continuously changing as the free variable changes. The

significant sharp edge of pHs in both plots defines the ion balance condition. We selected the observations data

obtained during the pollution episodes within the RH ranging from 50% to 70% to compare with the results of both

sensitivity tests. As shown in Fig.10, apart from some data points (those with lower nitrate concentration but very

340   high NH_x concentration), observation data (triangle points) are quite well merged into the results of sensitivity tests,

and the pH values are generally higher than the test results due to the lack of crustal ions inputting the sensitivity

simulation. Therefore, the result of sensitivity tests can well represent the pH change of the real atmosphere

environment in Beijing.

Future changes in particle pH can be found with the sensitivity test results. Cutting down the sulfate

345   concentration without reducing atmospheric ammonia (horizontally moving from right to left in Fig. 10, left part)

can lead to a significant increase of particle pH (up to 5). As can be seen from the right part of Fig.10, the elevation

of particle pH might be enhanced with the help of more nitrate in $PM_{2.5}$. The effect of nitrate on particle pH greatly

relies on the NH_x concentration in the atmosphere. As the ammonia in the atmosphere over North China might still be increasing (Liu et al. 2018), and the sulfur content in the atmosphere might not be greatly reduced in the future,

350   the particle pH shall increase in the path along the ion balance edge, which also implies a synergetic effect of increased nitrate and ammonia.

These results (lower acidity, higher hygroscopicity) provide insights into the possible effects of an elevated nitrate content on the physiochemical properties of particles. First, heterogeneous reactions that don't need high acidity might greatly contribute to the airborne particle chemistry, such as the NO_2-induced oxidation of SO_2

355   mechanism (Cheng et al. 2016; Wang et al. 2016). Reactions which rely greatly on acidified particles might contribute less, such as the acid-catalyzed SOA formation from VOCs (Jang et al. 2002; Surratt et al. 2010). Second, the uptake processes of gaseous compounds onto particles (carbonyl acids, for example) might be enhanced, and the uptake of alkaline compounds could also be enhanced via the ALWC elevation. Third, optical properties of particles will greatly vary. On one hand, higher ALWC can increase the light scattering effect (Titos et al. 2014), while the

360   light absorption by BrC would be enhanced at higher pH (Phillips et al. 2017). All these facts might add up the difficulties to the control of moderate haze in Beijing, which usually occurs with lower RH and higher nitrate content as shown in this study. It is strongly suggested that the control strategy should be made accordingly based on thorough and scientific evaluation on both NO_x and ammonia.

5 Conclusions

365   Due to the strict emission controls, $PM_{2.5}$ in Beijing during the winter of 2017 greatly decreased to a low level (39.7 μg m^{-3} for daily average concentration), but moderate haze episodes still frequently occurred in the city. With the observation and historical data, we found that the SO_2 concentration decreased significantly while the NO_2 concentration far exceeded that of SO_2 and kept increasing in Beijing during winter. In response to the emission control, the nitrate concentration exceeded the concentration of sulfate significantly and thus became the dominant

370   SIA component in fine particles. The molar ratio of nitrate to sulfate kept increasing over the years and rose to 2.7

during $PM_{2.5}$ pollution episodes in the winter of 2017. The ammonium to sulfate ratio has always been above 1.5 in Beijing, and has exceeded 3 since 2011. Such a sufficient ammonia is favorable for the nitrate formation in Beijing. During the campaign the pH of $PM_{2.5}$ increased from 4.4 to 5.4 as the molar ratio of nitrate to sulfate increased from 1 to 5, which is firstly due to the less amount of sulfate that suppressed the formation of H^+ and secondly due to the

375   ammonia neutralizing.

      Sensitivity tests of particle hygroscopicity and acidity were conducted to investigate the possible changes in the physiochemical properties if ammonia and nitrate are not well controlled in China in the future. The results showed that the nitrate-rich particles can absorb more water than particles with higher sulfate fractions under a moderate humid conditions (RH<60%), and the particle pH increases rapidly due to the synergetic effect of ammonia and

380   nitrate, which will very likely occur in China in the following years, because both the pollutants are not well controlled yet. Those changes will enhance the uptake of gaseous compounds, promote the chemical reactions which favor lower acidity, and also affect the optical properties of airborne particles in China. Therefore, the processes and properties of haze particles during nitrated-dominated periods in the country need to be thoroughly investigated with more consideration on the more hygroscopic and neutralized particles.

385   **Author contribution**

    G.H. Wang conceived the study and designed the experiment. YN. Xie conducted the online IGAC-$PM_{2.5}$ chemical composition analysis and filter sampling in Beijing during the campaign. GQ. Tang, LL. Wang, YS. Wang and J. Gao provided other related observation data used in this article, including trace gases, PM mass concentrations, meteorological data. G.H. Wang, XP. Wang, YB. Chen, GY. Xue and SS. Ge conducted the lab analysis of filters

390   and the data QA/QC. YN. Xie, G.H. Wang and J.M. Chen performed the data analysis. YN. Xie and G.H. Wang wrote the paper. All the co-authors contributed to the data interpretation and discussion

Acknowledgements

This work was financially supported by the National Key R&D Program of China (2017YFC0210000), and the National Nature Science Foundation of China (No. 41773117). We thank Mr. Yicheng, Lin and Mr. Zhenrong

395 Huang from Fortelice International Co., Ltd. for their technical supporting in IGAC operation during the campaign.

References

Badger, C. L., Griffiths, P. T., George, I., Abbatt, J. P. D., and Cox, R. A.: Reactive Uptake of N_2O_5 by Aerosol Particles Containing Mixtures of Humic Acid and Ammonium Sulfate, J. Phys. Chem., 110, 6986-6994,

400 10.1021/jp0562678, 2006.

Bertram, T. H., and Thornton, J. A.: Toward a general parameterization of N2O5 reactivity on aqueous particles: the competing effects of particle liquid water, nitrate and chloride, Atmos. Chem. Phys., 9, 8351-8363, 10.5194/acp-9-8351-2009, 2009.

Cao, J.-J., Shen, Z.-X., Chow, J. C., Watson, J. G, Lee, S.-C., Tie, X.-X., Ho, K.-F., Wang, G.-H., and Han, Y.-M.:

405 Winter and Summer $PM_{2.5}$ Chemical Compositions in Fourteen Chinese Cities, J. Air. Waste. Manage., 62, 1214-1226, 10.1080/10962247.2012.701193, 2012.

Chen, J. M., Li, C. L., Ristovski, Z., Milic, A., Gu, Y. T., Islam, M. S., Wang, S. X., Hao, J. M., Zhang, H. F., He, C. R., Guo, H., Fu, H. B., Miljevic, B., Morawska, L., Thai, P., Fat, L., Pereira, G., Ding, A. J., Huang, X., and Dumka, U. C.: A review of biomass burning: Emissions and impacts on air quality, health and climate in China,

410 Sci. Total Environ., 579, 1000-1034, 10.1016/j.scitotenv.2016.11.025, 2017.

Chen, T., Chu, B., Ge, Y., Zhang, S., Ma, Q., He, H., and Li, S.-M.: Enhancement of aqueous sulfate formation by the coexistence of NO2/NH3 under high ionic strengths in aerosol water, Environmental Pollution, 252, 236-244, 10.1016/j.envpol.2019.05.119, 2019.

Cheng, J., Su, J., Cui, T., Li, X., Dong, X., Sun, F., Yang, Y., Tong, D., Zheng, Y., Li, J., Zhang, Q., and He, K.:

415   Dominant role of emission reduction in $PM_{2.5}$ air quality improvement in Beijing during 2013-2017: a model-based decomposition analysis, Atmos. Chem. Phys. Discuss., 2018, 1-31, 10.5194/acp-2018-1145, 2018.

Cheng, Y., Zheng, G., Wei, C., Mu, Q., Zheng, B., Wang, Z., Gao, M., Zhang, Q., He, K., Carmichael, G., Pöschl, U., and Su, H.: Reactive nitrogen chemistry in aerosol water as a source of sulfate during haze events in China, Sci. Adv., 2, e1601530, 10.1126/sciadv.1601530, 2016.

420   Clegg, S. L., Kleeman, M. J., Griffin, R. J., and Seinfeld, J. H.: Effects of uncertainties in the thermodynamic properties of aerosol components in an air quality model Part 1: Treatment of inorganic electrolytes and organic compounds in the condensed phase, Atmos. Chem. Phys., 8, 1057-1085, 10.5194/acp-8-1057-2008, 2008.

de Foy, B., Lu, Z., and Streets, D. G.: Satellite NO_2 retrievals suggest China has exceeded its NO_x reduction goals from the twelfth Five-Year Plan, Sci. Rep., 6, 35912, 10.1038/srep35912, 2016.

425   Ding, A. J., Fu, C. B., Yang, X. Q., Sun, J. N., Zheng, L. F., Xie, Y. N., Herrmann, E., Nie, W., Petäjä, T., Kerminen, V. M., and Kulmala, M.: Ozone and fine particle in the western Yangtze River Delta: an overview of 1 yr data at the SORPES station, Atmos. Chem. Phys., 13, 5813-5830, 10.5194/acp-13-5813-2013, 2013.

Elser, M., Huang, R. J., Wolf, R., Slowik, J. G., Wang, Q., Canonaco, F., Li, G., Bozzetti, C., Daellenbach, K. R., Huang, Y., Zhang, R., Li, Z., Cao, J., Baltensperger, U., El-Haddad, I., and Prévôt, A. S. H.: New insights into

430   PM2.5 chemical composition and sources in two major cities in China during extreme haze events using aerosol mass spectrometry, Atmos. Chem. Phys., 16, 3207-3225, 10.5194/acp-16-3207-2016, 2016.

Ervens, B., George, C., Williams, J. E., Buxton, G. V., Salmon, G. A., Bydder, M., Wilkinson, F., Dentener, F., Mirabel, P., Wolke, R., and Herrmann, H.: CAPRAM 2.4 (MODAC mechanism): An extended and condensed tropospheric aqueous phase mechanism and its application, J. Geophys. Res-Atmos., 108, 10.1029/2002JD002202,

435   2003.

Fountoukis, C., and Nenes, A.: ISORROPIA II: a computationally efficient thermodynamic equilibrium model for K^+ - Ca^{2+} - Mg^{2+} - NH_4^+ - Na^+ - SO_4^{2-} - NO_3^- - Cl^- - H_2O aerosols, Atmos. Chem. Phys., 7, 4639-4659, 10.5194/acp-7-4639-2007, 2007.

Freedman, M. A., Ott, E.-J. E., and Marak, K. E.: Role of pH in Aerosol Processes and Measurement Challenges, J. Phys. Chem., 123, 1275-1284, 10.1021/acs.jpca.8b10676, 2019.

Ge, S., Wang, G., Zhang, S., Li, D., Xie, Y., Wu, C., Yuan, Q., Chen, J., and Zhang, H.: Abundant NH_3 in China Enhances Atmospheric HONO Production by Promoting the Heterogeneous Reaction of SO_2 with NO_2, Environ. Sci. Technol., 53, 14339-14347, 10.1021/acs.est.9b04196, 2019.

Ge, X., He, Y., Sun, Y., Xu, J., Wang, J., Shen, Y., and Chen, M.: Characteristics and Formation Mechanisms of Fine Particulate Nitrate in Typical Urban Areas in China, Atmosphere-Basel., 8, 10.3390/atmos8030062, 2017.

Ge, Z., Wexler, A. S., and Johnston, M. V.: Multicomponent Aerosol Crystallization, J. Colloid. Interf. Sci., 183, 68-77, 10.1006/jcis.1996.0519, 1996.

Ge, Z., Wexler, A. S., and Johnston, M. V.: Deliquescence Behavior of Multicomponent Aerosols, J. Phys. Chem., 102, 173-180, 10.1021/jp972396f, 1998.

Guo, H., Sullivan, A. P., Campuzano-Jost, P., Schroder, J. C., Lopez-Hilfiker, F. D., Dibb, J. E., Jimenez, J. L., Thornton, J. A., Brown, S. S., Nenes, A., and Weber, R. J.: Fine particle pH and the partitioning of nitric acid during winter in the northeastern United States, J. Geophys. Res-Atmos., 121, 10,355-310,376, 10.1002/2016JD025311, 2016.

Guo, H., Weber, R. J., and Nenes, A.: High levels of ammonia do not raise fine particle pH sufficiently to yield nitrogen oxide-dominated sulfate production, Sci. Rep., 7, 12109, 10.1038/s41598-017-11704-0, 2017.

Guo, S., Hu, M., Zamora, M. L., Peng, J., Shang, D., Zheng, J., Du, Z., Wu, Z., Shao, M., Zeng, L., Molina, M. J., and Zhang, R.: Elucidating severe urban haze formation in China, P. Natl. Acad. Sci. USA., 111, 17373, 10.1073/pnas.1419604111, 2014.

He, K., Yang, F., Ma, Y., Zhang, Q., Yao, X., Chan, C. K., Cadle, S., Chan, T., and Mulawa, P.: The characteristics of $PM_{2.5}$ in Beijing, China, Atmos. Environ., 35, 4959-4970, 10.1016/S1352-2310(01)00301-6, 2001.

He, P., Alexander, B., Geng, L., Chi, X., Fan, S., Zhan, H., Kang, H., Zheng, G., Cheng, Y., Su, H., Liu, C., and Xie, Z.: Isotopic constraints on heterogeneous sulfate production in Beijing haze, Atmos. Chem. Phys., 18, 5515-5528,

10.5194/acp-18-5515-2018, 2018.

Herrmann, H., Tilgner, A., Barzaghi, P., Majdik, Z., Gligorovski, S., Poulain, L., and Monod, A.: Towards a more detailed description of tropospheric aqueous phase organic chemistry: CAPRAM 3.0, Atmos. Environ., 39, 4351-4363, 10.1016/j.atmosenv.2005.02.016, 2005.

Hodas, N., Sullivan, A. P., Skog, K., Keutsch, F. N., Collett, J. L., Decesari, S., Facchini, M. C., Carlton, A. G., Laaksonen, A., and Turpin, B. J.: Aerosol Liquid Water Driven by Anthropogenic Nitrate: Implications for Lifetimes of Water-Soluble Organic Gases and Potential for Secondary Organic Aerosol Formation, Environ. Sci. Technol., 48, 11127-11136, 10.1021/es5025096, 2014.

Huang, R.-J., Zhang, Y., Bozzetti, C., Ho, K.-F., Cao, J.-J., Han, Y., Daellenbach, K. R., Slowik, J. G., Platt, S. M., Canonaco, F., Zotter, P., Wolf, R., Pieber, S. M., Bruns, E. A., Crippa, M., Ciarelli, G., Piazzalunga, A., Schwikowski, M., Abbaszade, G., Schnelle-Kreis, J., Zimmermann, R., An, Z., Szidat, S., Baltensperger, U., Haddad, I. E., and Prévôt, A. S. H.: High secondary aerosol contribution to particulate pollution during haze events in China, Nature, 514, 218, 10.1038/nature13774, 2014a.

Huang, X., Song, Y., Zhao, C., Li, M., Zhu, T., Zhang, Q., and Zhang, X.: Pathways of sulfate enhancement by natural and anthropogenic mineral aerosols in China, J. Geophys. Res-Atmos., 119, 14,165-114,179, 10.1002/2014JD022301, 2014b.

Huang, X., Liu, Z., Liu, J., Hu, B., Wen, T., Tang, G., Zhang, J., Wu, F., Ji, D., Wang, L., and Wang, Y.: Chemical characterization and source identification of $PM_{2.5}$ at multiple sites in the Beijing–Tianjin–Hebei region, China, Atmos. Chem. Phys., 17, 12941-12962, 10.5194/acp-17-12941-2017, 2017.

Jang, M., Czoschke, N. M., Lee, S., and Kamens, R. M.: Heterogeneous Atmospheric Aerosol Production by Acid-Catalyzed Particle-Phase Reactions, Science, 298, 814, 10.1126/science.1075798, 2002.

Ji, D., Li, L., Wang, Y., Zhang, J., Cheng, M., Sun, Y., Liu, Z., Wang, L., Tang, G., Hu, B., Chao, N., Wen, T., and Miao, H.: The heaviest particulate air-pollution episodes occurred in northern China in January, 2013: Insights gained from observation, Atmos. Environ., 92, 546-556, 10.1016/j.atmosenv.2014.04.048, 2014.

Ji, D., Cui, Y., Li, L., He, J., Wang, L., Zhang, H., Wang, W., Zhou, L., Maenhaut, W., Wen, T., and Wang, Y.: Characterization and source identification of fine particulate matter in urban Beijing during the 2015 Spring Festival, Sci. Total Environ., 628-629, 430-440, 10.1016/j.scitotenv.2018.01.304, 2018.

490 Lang, J., Zhang, Y., Zhou, Y., Cheng, S., Chen, D., Guo, X., Chen, S., Li, X., Xing, X., and Wang, H.: Trends of $PM_{2.5}$ and Chemical Composition in Beijing, 2000 - 2015, Aerosol. Air. Qual. Res., 17, 412-425, 10.4209/aaqr.2016.07.0307, 2017.

Liu, F., Zhang, Q., van der A, R. J., Zheng, B., Tong, D., Yan, L., Zheng, Y., and He, K.: Recent reduction in NO_x emissions over China: synthesis of satellite observations and emission inventories, Environ. Res. Lett., 11, 114002, 495 10.1088/1748-9326/11/11/114002, 2016.

Liu, M., Song, Y., Zhou, T., Xu, Z., Yan, C., Zheng, M., Wu, Z., Hu, M., Wu, Y., and Zhu, T.: Fine particle pH during severe haze episodes in northern China, Geophys. Res. Lett., 44, 5213-5221, 10.1002/2017GL073210, 2017.

Liu, M., Huang, X., Song, Y., Xu, T., Wang, S., Wu, Z., Hu, M., Zhang, L., Zhang, Q., Pan, Y., Liu, X., and Zhu, T.: 500 Rapid SO_2 emission reductions significantly increase tropospheric ammonia concentrations over the North China Plain, Atmos. Chem. Phys., 18, 17933-17943, 10.5194/acp-18-17933-2018, 2018.

Liu, M., Huang, X., Song, Y., Tang, J., Cao, J., Zhang, X., Zhang, Q., Wang, S., Xu, T., Kang, L., Cai, X., Zhang, H., Yang, F., Wang, H., Yu, J. Z., Lau, A. K. H., He, L., Huang, X., Duan, L., Ding, A., Xue, L., Gao, J., Liu, B., and Zhu, T.: Ammonia emission control in China would mitigate haze pollution and nitrogen deposition, but 505 worsen acid rain, P. Natl. Acad. Sci. USA., 116, 7760, 10.1073/pnas.1814880116, 2019.

Mauer, L. J., and Taylor, L. S.: Water-Solids Interactions: Deliquescence, Annu. Rev. Food. Sci. T., 1, 41-63, 10.1146/annurev.food.080708.100915, 2010.

Murphy, J. G., Gregoire, P. K., Tevlin, A. G., Wentworth, G. R., Ellis, R. A., Markovic, M. Z., and VandenBoer, T. C.: Observational constraints on particle acidity using measurements and modelling of particles and gases, Faraday 510 Discussions, 200, 379-395, 10.1039/C7FD00086C, 2017.

Pathak, R. K., Yao, X., and Chan, C. K.: Sampling Artifacts of Acidity and Ionic Species in PM2.5, Environ. Sci. Technol., 38, 254-259, 10.1021/es0342244, 2004.

Pathak, R. K., Wu, W. S., and Wang, T.: Summertime $PM_{2.5}$ ionic species in four major cities of China: nitrate formation in an ammonia-deficient atmosphere, Atmos. Chem. Phys., 9, 1711-1722, 10.5194/acp-9-1711-2009, 2009.

Pathak, R. K., Wang, T., and Wu, W. S.: Nighttime enhancement of $PM_{2.5}$ nitrate in ammonia-poor atmospheric conditions in Beijing and Shanghai: Plausible contributions of heterogeneous hydrolysis of N_2O_5 and HNO_3 partitioning, Atmos. Environ., 45, 1183-1191, 10.1016/j.atmosenv.2010.09.003, 2011.

Phillips, S. M., Bellcross, A. D., and Smith, G. D.: Light Absorption by Brown Carbon in the Southeastern United States is pH-dependent, Environ. Sci. Technol., 51, 6782-6790, 10.1021/acs.est.7b01116, 2017.

Robert, O., Mateusz, R., and Marek, B.: Impact of Use of Chemical Transformation Modules in Calpuff on the Results of Air Dispersion Modelling, Ecol. Chem. Eng. S., 23, 605-620, 10.1515/eces-2016-0043, 2016.

Shah, V., Jaeglé, L., Thornton, J. A., Lopez-Hilfiker, F. D., Lee, B. H., Schroder, J. C., Campuzano-Jost, P., Jimenez, J. L., Guo, H., Sullivan, A. P., Weber, R. J., Green, J. R., Fiddler, M. N., Bililign, S., Campos, T. L., Stell, M., Weinheimer, A. J., Montzka, D. D., and Brown, S. S.: Chemical feedbacks weaken the wintertime response of particulate sulfate and nitrate to emissions reductions over the eastern United States, P. Natl. Acad. Sci. USA., 115, 8110, 10.1073/pnas.1803295115, 2018.

Shao, P., Tian, H., Sun, Y., Liu, H., Wu, B., Liu, S., Liu, X., Wu, Y., Liang, W., Wang, Y., Gao, J., Xue, Y., Bai, X., Liu, W., Lin, S., and Hu, G.: Characterizing remarkable changes of severe haze events and chemical compositions in multi-size airborne particles (PM_1, $PM_{2.5}$ and PM_{10}) from January 2013 to 2016-2017 winter in Beijing, China, Atmos. Environ., 189, 133-144, 10.1016/j.atmosenv.2018.06.038, 2018.

Shi, G., Xu, J., Peng, X., Xiao, Z., Chen, K., Tian, Y., Guan, X., Feng, Y., Yu, H., Nenes, A., and Russell, A. G.: pH of Aerosols in a Polluted Atmosphere: Source Contributions to Highly Acidic Aerosol, Environ. Sci. Technol., 51, 4289-4296, 10.1021/acs.est.6b05736, 2017.

535   Shi, X., Nenes, A., Xiao, Z., Song, S., Yu, H., Shi, G., Zhao, Q., Chen, K., Feng, Y., and Russell, A. G.: High-Resolution Data Sets Unravel the Effects of Sources and Meteorological Conditions on Nitrate and Its Gas-Particle Partitioning, Environ. Sci. Technol., 53, 3048-3057, 10.1021/acs.est.8b06524, 2019.

Song, S., Gao, M., Xu, W., Shao, J., Shi, G., Wang, S., Wang, Y., Sun, Y., and McElroy, M. B.: Fine-particle pH for Beijing winter haze as inferred from different thermodynamic equilibrium models, Atmos. Chem. Phys., 18,
540   7423-7438, 10.5194/acp-18-7423-2018, 2018.

Sun, P., Nie, W., Chi, X., Xie, Y., Huang, X., Xu, Z., Qi, X., Xu, Z., Wang, L., Wang, T., Zhang, Q., and Ding, A.: Two years of online measurement of fine particulate nitrate in the western Yangtze River Delta: influences of thermodynamics and N_2O_5 hydrolysis, Atmos. Chem. Phys., 18, 17177-17190, 10.5194/acp-18-17177-2018, 2018.

Surratt, J. D., Chan, A. W. H., Eddingsaas, N. C., Chan, M., Loza, C. L., Kwan, A. J., Hersey, S. P., Flagan, R. C.,
545   Wennberg, P. O., and Seinfeld, J. H.: Reactive intermediates revealed in secondary organic aerosol formation from isoprene, P. Natl. Acad. Sci. USA., 107, 6640, 10.1073/pnas.0911114107, 2010.

Tan, Z., Rohrer, F., Lu, K., Ma, X., Bohn, B., Broch, S., Dong, H., Fuchs, H., Gkatzelis, G. I., Hofzumahaus, A., Holland, F., Li, X., Liu, Y., Liu, Y., Novelli, A., Shao, M., Wang, H., Wu, Y., Zeng, L., Hu, M., Kiendler-Scharr, A., Wahner, A., and Zhang, Y.: Wintertime photochemistry in Beijing: observations of RO_x radical concentrations in
550   the North China Plain during the BEST-ONE campaign, Atmos. Chem. Phys., 18, 12391-12411, 10.5194/acp-18-12391-2018, 2018.

Tao, Y., and Murphy, J. G.: The sensitivity of PM2.5 acidity to meteorological parameters and chemical composition changes: 10-year records from six Canadian monitoring sites, Atmos. Chem. Phys. Discuss., 2019, 1-21, 10.5194/acp-2019-238, 2019.

555   ten Brink, H. M., and Veefkind, J. P.: Humidity dependence of the light-scattering by ammonium nitrate, J. Aerosol. Sci., 26, S553-S554, 10.1016/0021-8502(95)97184-G, 1995.

Titos, G., Jefferson, A., Sheridan, P. J., Andrews, E., Lyamani, H., Alados-Arboledas, L., and Ogren, J. A.: Aerosol light-scattering enhancement due to water uptake during the TCAP campaign, Atmos. Chem. Phys., 14, 7031-7043,

10.5194/acp-14-7031-2014, 2014.

Wang, G., Zhang, R., Gomez, M. E., Yang, L., Levy Zamora, M., Hu, M., Lin, Y., Peng, J., Guo, S., Meng, J., Li, J., Cheng, C., Hu, T., Ren, Y., Wang, Y., Gao, J., Cao, J., An, Z., Zhou, W., Li, G., Wang, J., Tian, P., Marrero-Ortiz, W., Secrest, J., Du, Z., Zheng, J., Shang, D., Zeng, L., Shao, M., Wang, W., Huang, Y., Wang, Y., Zhu, Y., Li, Y., Hu, J., Pan, B., Cai, L., Cheng, Y., Ji, Y., Zhang, F., Rosenfeld, D., Liss, P. S., Duce, R. A., Kolb, C. E., and Molina, M. J.: Persistent sulfate formation from London Fog to Chinese haze, P. NATL. ACAD. SCI. USA, 113, 13630, 10.1073/pnas.1616540113, 2016.

Wang, G., Zhang, F., Peng, J., Duan, L., Ji, Y., Marrero-Ortiz, W., Wang, J., Li, J., Wu, C., Cao, C., Wang, Y., Zheng, J., Secrest, J., Li, Y., Wang, Y., Li, H., Li, N., and Zhang, R.: Particle acidity and sulfate production during severe haze events in China cannot be reliably inferred by assuming a mixture of inorganic salts, Atmos. Chem. Phys., 18, 10123-10132, 10.5194/acp-18-10123-2018, 2018a.

Wang, H., Lu, K., Chen, X., Zhu, Q., Chen, Q., Guo, S., Jiang, M., Li, X., Shang, D., Tan, Z., Wu, Y., Wu, Z., Zou, Q., Zheng, Y., Zeng, L., Zhu, T., Hu, M., and Zhang, Y.: High N_2O_5 Concentrations Observed in Urban Beijing: Implications of a Large Nitrate Formation Pathway, Environ. Sci. Technol. Let., 4, 416-420, 10.1021/acs.estlett.7b00341, 2017.

Wang, T., Wang, P., Theys, N., Tong, D., Hendrick, F., Zhang, Q., and Van Roozendael, M.: Spatial and temporal changes in SO_2 regimes over China in the recent decade and the driving mechanism, Atmos. Chem. Phys., 18, 18063-18078, 10.5194/acp-18-18063-2018, 2018b.

Wang, X., Shen, X. J., Sun, J. Y., Zhang, X. Y., Wang, Y. Q., Zhang, Y. M., Wang, P., Xia, C., Qi, X. F., and Zhong, J. T.: Size-resolved hygroscopic behavior of atmospheric aerosols during heavy aerosol pollution episodes in Beijing in December 2016, Atmos. Environ., 194, 188-197, 10.1016/j.atmosenv.2018.09.041, 2018c.

Wang, Y., Zhang, Q. Q., He, K., Zhang, Q., and Chai, L.: Sulfate-nitrate-ammonium aerosols over China: response to 2000–2015 emission changes of sulfur dioxide, nitrogen oxides, and ammonia, Atmos. Chem. Phys., 13, 2635-2652, 10.5194/acp-13-2635-2013, 2013.

Wang, Y., Zhang, Q., Jiang, J., Zhou, W., Wang, B., He, K., Duan, F., Zhang, Q., Philip, S., and Xie, Y.: Enhanced sulfate formation during China's severe winter haze episode in January 2013 missing from current models, J. Geophys. Res-Atmos., 119, 10,425-410,440, 10.1002/2013JD021426, 2014.

Weber, R. J., Guo, H., Russell, A. G., and Nenes, A.: High aerosol acidity despite declining atmospheric sulfate concentrations over the past 15 years, Nat. Geosci., 9, 282, 10.1038/ngeo2665, 2016.

Wei, H., Vejerano, E. P., Leng, W., Huang, Q., Willner, M. R., Marr, L. C., and Vikesland, P. J.: Aerosol microdroplets exhibit a stable pH gradient, P. Natl. Acad. Sci. USA., 115, 7272, 10.1073/pnas.1720488115, 2018.

Wexler, A. S., and Seinfeld, J. H.: Second-generation inorganic aerosol model, Atmos. Environ. A-Gen, 25, 2731-2748, 10.1016/0960-1686(91)90203-J, 1991.

Willeke, K., Society, A. C., and Kagakkai, N.: Generation of Aerosols and Facilities for Exposure Experiments, Ann Arbor Science, 1980.

Xie, Y., Ding, A., Nie, W., Mao, H., Qi, X., Huang, X., Xu, Z., Kerminen, V.-M., Petäjä, T., Chi, X., Virkkula, A., Boy, M., Xue, L., Guo, J., Sun, J., Yang, X., Kulmala, M., and Fu, C.: Enhanced sulfate formation by nitrogen dioxide: Implications from in situ observations at the SORPES station, J. Geophys. Res-Atmos., 120, 12679-12694, 10.1002/2015JD023607, 2015.

Xue, J., Griffith, S. M., Yu, X., Lau, A. K. H., and Yu, J. Z.: Effect of nitrate and sulfate relative abundance in $PM_{2.5}$ on liquid water content explored through half-hourly observations of inorganic soluble aerosols at a polluted receptor site, Atmos. Environ., 99, 24-31, 10.1016/j.atmosenv.2014.09.049, 2014.

Xue, J., Yu, X., Yuan, Z., Griffith, S. M., Lau, A. K. H., Seinfeld, J. H., and Yu, J. Z.: Efficient control of atmospheric sulfate production based on three formation regimes, Nat. Geosci., 12, 977-982, 10.1038/s41561-019-0485-5, 2019.

Young, L.-H., Li, C.-H., Lin, M.-Y., Hwang, B.-F., Hsu, H.-T., Chen, Y.-C., Jung, C.-R., Chen, K.-C., Cheng, D.-H., Wang, V.-S., Chiang, H.-C., and Tsai, P.-J.: Field performance of a semi-continuous monitor for ambient $PM_{2.5}$ water-soluble inorganic ions and gases at a suburban site, Atmos. Environ., 144, 376-388,

10.1016/j.atmosenv.2016.08.062, 2016.

Yu, S., Dennis, R., Roselle, S., Nenes, A., Walker, J., Eder, B., Schere, K., Swall, J., and Robarge, W.: An assessment of the ability of three-dimensional air quality models with current thermodynamic equilibrium models

610   to predict aerosol NO_3^-, J. Geophys. Res-Atmos., 110, 10.1029/2004JD004718, 2005.

Zhang, Q., He, K., and Huo, H.: Cleaning China's air, Nature, 484, 161, 10.1038/484161a, 2012.

Zhang, Q., Quan, J. N., Tie, X. X., Li, X., Liu, Q., Gao, Y., and Zhao, D. L.: Effects of meteorology and secondary particle formation on visibility during heavy haze events in Beijing, China, Sci. Total Environ., 502, 578-584, 10.1016/j.scitotenv.2014.09.079, 2015.

615   Zhang, R., Wang, G., Guo, S., Zamora, M. L., Ying, Q., Lin, Y., Wang, W., Hu, M., and Wang, Y.: Formation of Urban Fine Particulate Matter, Chem. Rev., 115, 3803-3855, 10.1021/acs.chemrev.5b00067, 2015.
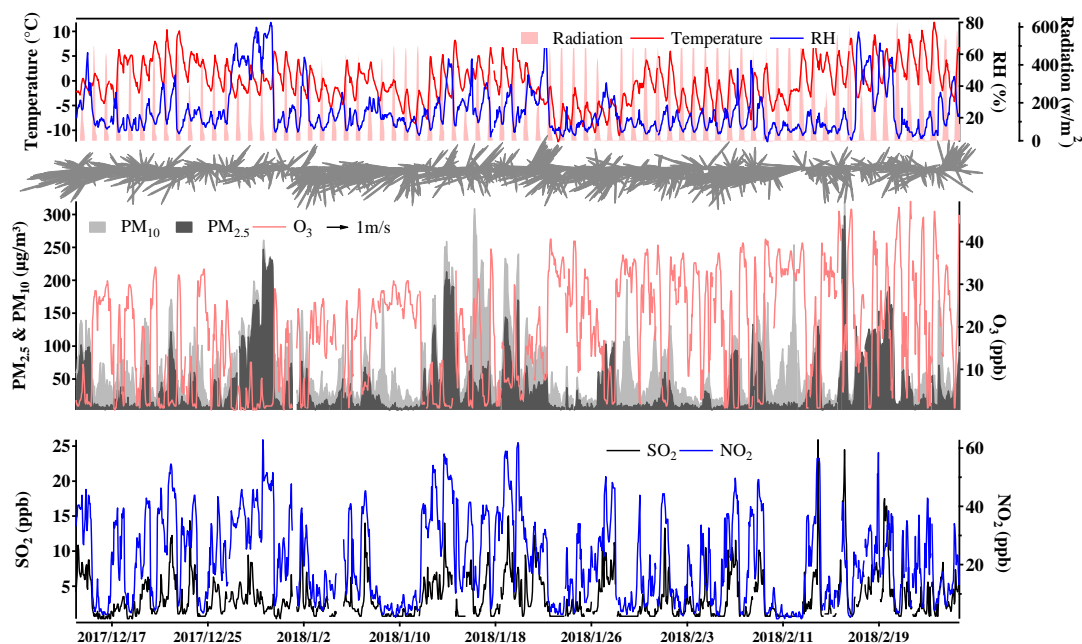
620   **FIG. 1. Timeseries of major pollutants during the campaign. Upper panel: radiation, temperature RH and wind arrows (drawn below); middle panel: PM$_{2.5}$, PM$_{10}$ and ozone concentration; lower panel: SO$_2$ and NO$_2$ concentrations.**
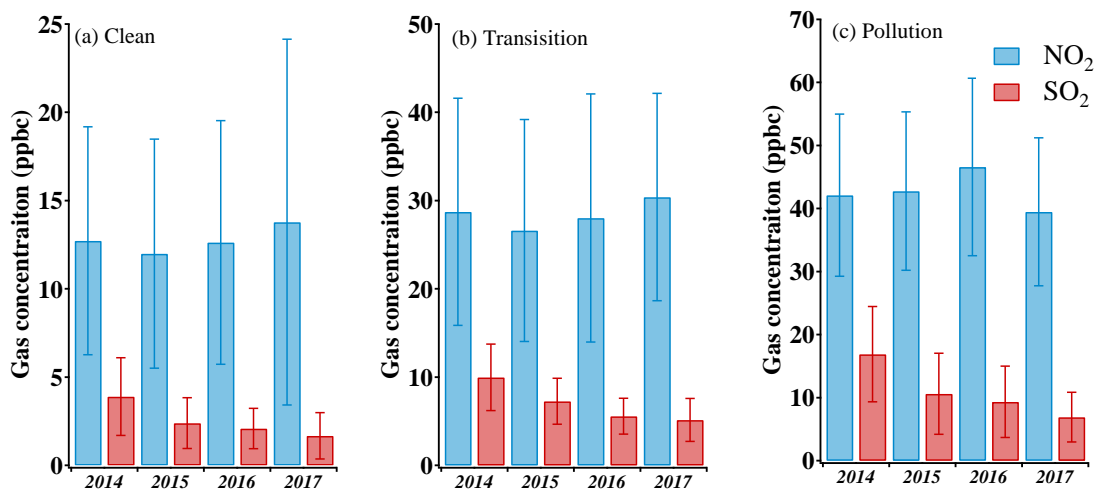
FIG. 2. Statistics plot of NO₂ and SO₂ measured in downtown of Beijing at different PM₂.₅ levels during winter (December–February) for the past 4 years. Historical data (2014–2016) are from air quality real-time publishing platform, China National Environmental Monitoring Center, and data of 2017 is obtained during the campaign.

625
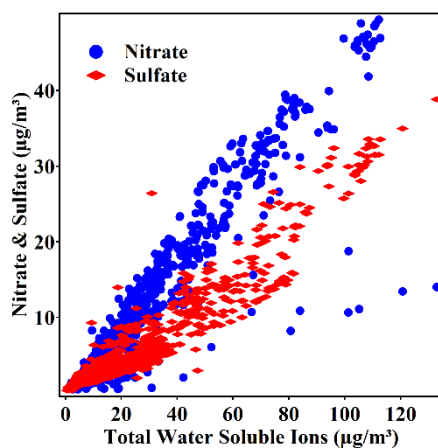
FIG. 3. Scatter plots of nitrate and sulfate vs. WSIs during the campaign.

630
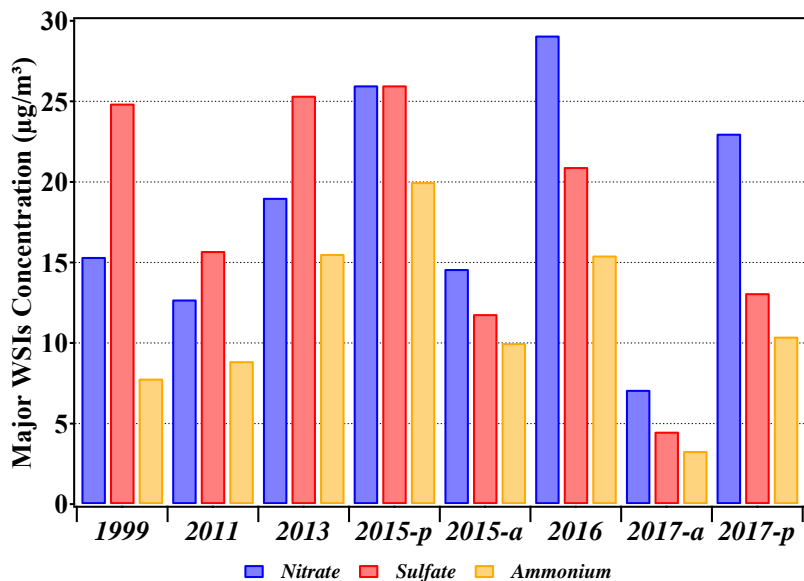
FIG. 4. Major inorganic compositions in PM$_{2.5}$ observed in Beijing during winter from representative articles. The results of 2017 denote the average concentration during haze episodes in this study. For details of the reviewed literature, please refer to Table S1.

635
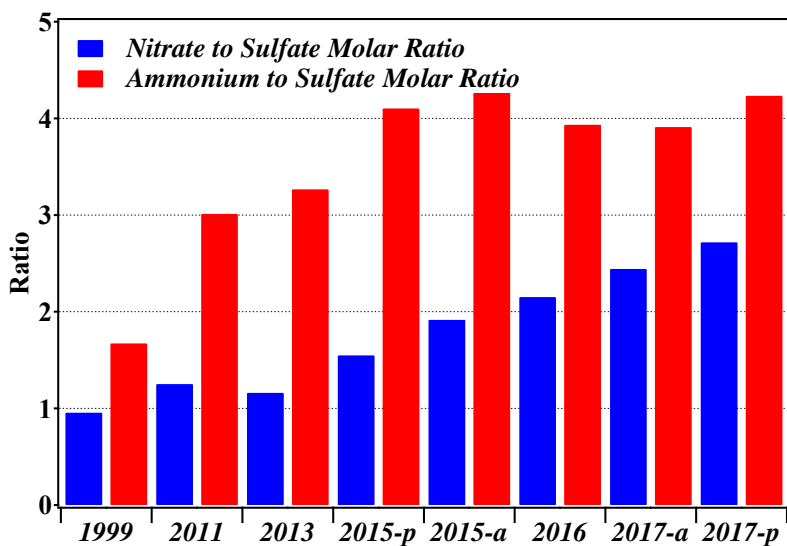
FIG. 5. Ratio$_{N-to-S}$ and Ratio$_{A-to-S}$ calculated from the averaged data reported in representative research articles. Only the data in pollution episodes is chosen for 2017.
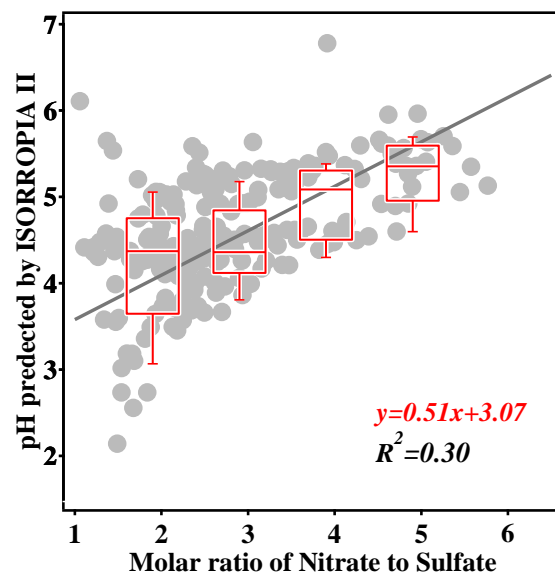
FIG. 6. Scatter plot of simulated pH vs. Ratio$_{N-to-S}$. Linear fitting and the correlation coefficient are given. The box plot denotes the data points classified by 4 different ranges of the Ratio$_{N-to-S}$: 0–2;2–3;3–4; and 4–6. Only the data corresponding to the pollution categories and with sufficient aerosol liquid water (above 5 µg m^{-3}) is chosen and the data during Chinese New Year is excluded.

640
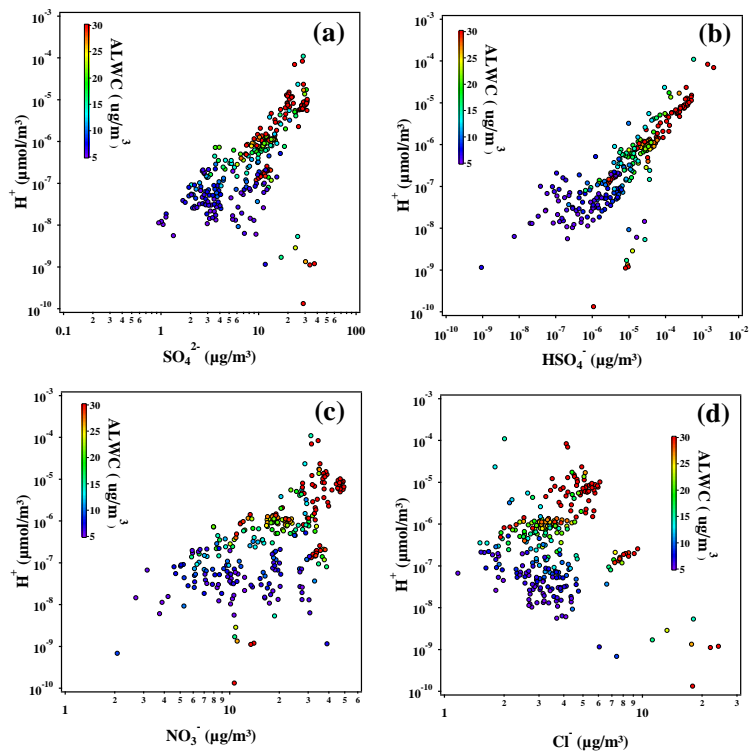
FIG. 7. Scatter plots of simulated H⁺ ion vs. major inorganic anions, including (a) SO₄²⁻, (b) HSO₄⁻, (c)NO₃⁻ and (d)Cl⁻;

645 **the coordinates are in logarithm. Only the data corresponding to the pollution categories and with sufficient aerosol**

liquid water (above 5 μg m⁻³) is chosen and the data during Chinese New Year is excluded.
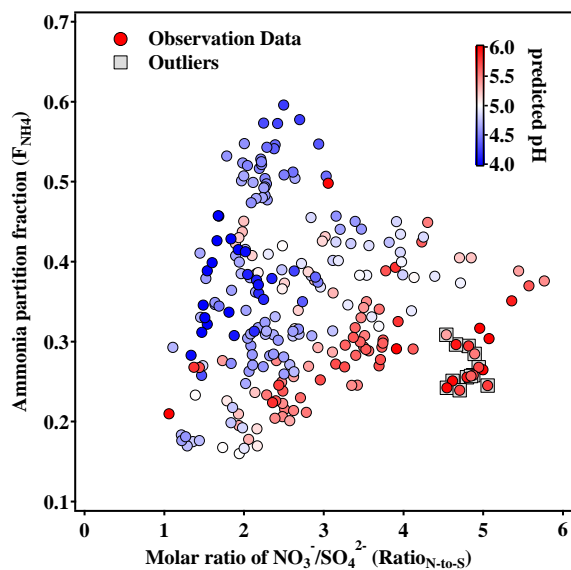
FIG. 8. Scatter plot of F_{NH4} vs. the Ratio$_{N-to-S}$ colored with predicted pH. Only the data corresponding to the pollution categories and with sufficient aerosol liquid water (above 5 µg m^{-3}) is chosen and the data during Chinese New Year is excluded. Note that the grey frame depicts the outliers which have lower F_{NH4} and lower Ammonia concentration.
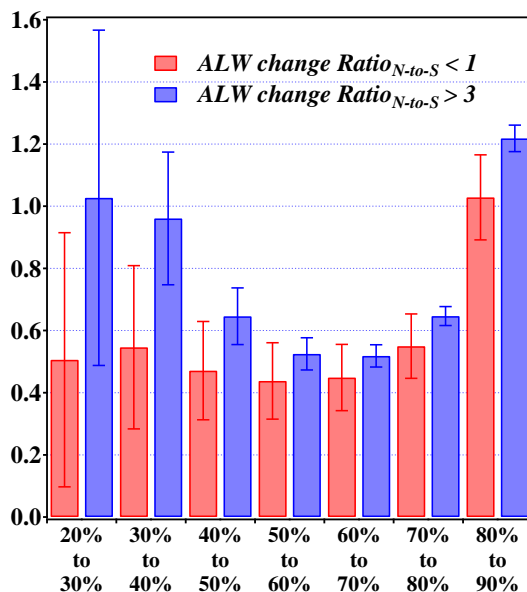
FIG. 9. Relative ALWC change due to the RH elevation at different Ratio$_{N-to-S}$. Bars represent the relative change amount, and whiskers depict the standard deviation.
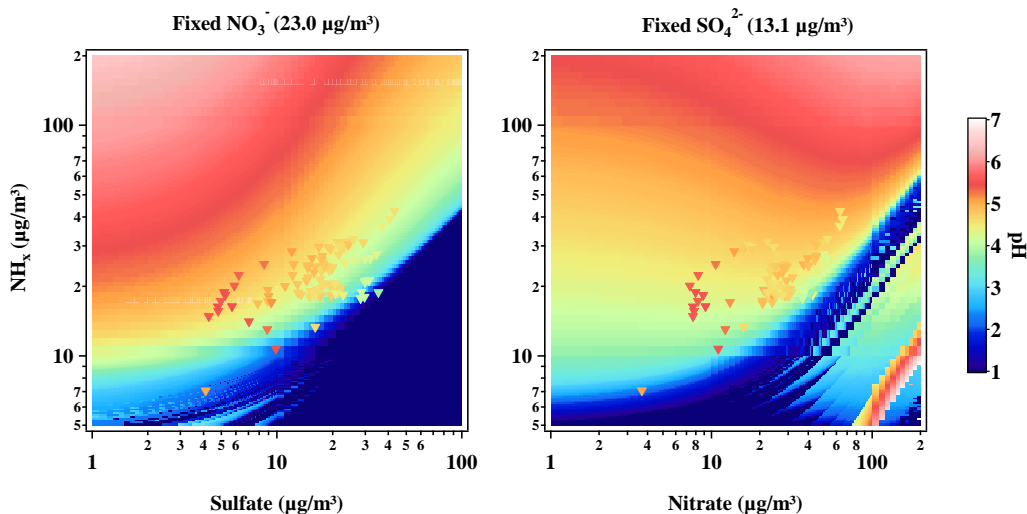
FIG. 10. Sensitivity tests of pH's response to sulfate or nitrate change with inputting given NH$_x$, simulated by

ISORROPIA II. Field measurement data (triangles) were drawn upon the simulation data and colored with predicted pH, respectively. The simulation is conducted with fixed RH (58%) and temperature (273.15 K).

Table 1. Visibility and concentrations of major pollutants in Beijing during the winter of 2017

	Average	Clean	Transition	Pollution
Visibility (km)	15±10	20±9.5	12±8.3	7.5±6.6
$PM_{2.5}$ ($\mu g/m^3$)	39.7±47.1	13.0±7.8	52.0±11.4	128±46.5
PM_{10} ($\mu g/m^3$)	68.5±53.9	42.2±27.9	99.2±43.3	153.3±52.1
O_3 (ppbv)	18.5±12.8	23.6±11.2	10.6±10.0	8.4±10.3
SO_2 (ppbv)	3.2±3.1	1.7±1.3	5.1±2.5	6.9±1.3
NO_2 (ppbv)	21.4±14.8	13.8±10.4	32.8±9.6	39.8±11.6

Table 2. Concentrations($\mu g/m^3$) of ammonia and inorganic ions of $PM_{2.5}$ measured by IGAC during the campaign

	Average	Clean	Transition	Pollution
NH_3	7.1±5.9	4.3±3.3	9.5±4.9	12.9±7.4
Na^+	0.3±0.3	0.2±0.4	0.4±0.2	0.5±0.2
NH_4^+	3.3±4.4	0.9±0.8	3.7±2.4	10.4±4.8
K^+	0.7±2.4	0.2±0.3	0.7±0.9	2.3±5.1
Mg^{2+}	0.2±0.5	0.2±0.6	0.2±0.1	0.4±0.7
Ca^{2+}	0.5±0.5	0.4±0.6	0.5±0.4	0.5±0.2
Cl^-	2.4±2.3	0.9±0.8	2.3±0.8	4.6±2.9
NO_3^-	7.1±9.6	1.7±1.4	7.9±3.2	23.0±10.7
SO_4^{2-}	4.5±5.9	1.8±1.6	4.2±2.2	13.1±8.4